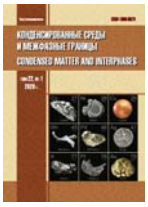

Condensed Matter and Interphases
(Kondensirovannye sredy i mezhfaznye granitsy)

Original articles

DOI: https://doi.org/10.17308/kcmf.2020.22/2525 eISSN 2687-0711
Received 04 February 2020
Accepted 15 March 2020
Published online 25 March 2020

Influence of a Weak Pulsed Electromagnetic Field on the Atomic Structure of Natural Aluminosilicates Clinoptilolite, Montmorillonite and Palygorskit

based on the materials of the XXIII All-Russian Conference with International Participation «X-ray and electron spectra and chemical bonds» (Voronezh, October 1–4, 2019)

©2020 L. I. Belchinskaya[a], K. V. Zhuzhukin[b], K. A. Barkov[b], S. A. Ivkov[b], V. A. Terekhov[b], E. P. Domashevskaya*[b]

[a]*Voronezh State Forestry University named G. F. Morozov, 8 Timiryazev str., Voronezh, Russian Federation*

[b]*Voronezh State University, 1 Universitetskaya pl., Voronezh 394018, Russian Federation*

Abstract

Natural and artificial aluminosilicates are relevant research objects due to their wide using in medicine, food and chemical industries, and in agriculture. The aim of the work is to study the possible changes under the influence of a weak pulsed electromagnetic field of the atomic structure of powdery samples of three minerals clinoptilolite $KNa_2Ca_2(Si_{29}Al_7)O_{72}\cdot 24H_2O$, montmorillonite $Ca_{0.2}(AlMg)_2Si_4O_{10}(OH)_2\cdot 4H_2O$ and palygorskite $MgAlSi_4O_{10}(OH)\cdot 4H_2O$, belonging to the group of natural aluminosilicates, in which silicon-oxygen and aluminum-oxygen tetrahedra are linked by a common oxygen atom. The results of studies by X-ray diffraction and ultra-soft X-ray emission spectroscopy showed that 48 hours after exposure of a weak pulsed electromagnetic field to 71 mT for 30 seconds, the atomic and electronic subsystems of mineral samples still kept changes.

The influence of a weak pulsed electromagnetic field on the atomic structure of minerals manifested itself differently in three samples in the form of one or two additional weak superstructural lines in diffractograms. The influence of a weak pulsed electromagnetic field on the local environment of silicon by oxygen atoms in silicon-oxygen tetrahedra was manifested in the form of changes in the fine structure of the ultra-soft X-ray emission spectroscopy silicon Si $L_{2,3}$ spectra, indicating the restoration of stoichiometry of silicon suboxides $SiO_{1.8}$ in the composition of aluminosilicates of the initial powders into stoichiometry equal to or close to silicon dioxide SiO_2, in all three minerals.

Keywords: aluminosilicates, clinoptilolite, montmorillonite, palygorskite, weak pulsed electromagnetic field, crystal structure, X-ray diffraction, ultra-soft X-ray emission spectra.

Fundings: This work was partially supported by the Ministry of Science and Education of the Russian Federation as part of the state assignment to universities in the field of scientific activity.

For citation: Belchinskaya L. I., Zhuzhukin K. V., Barkov K. A., Ivkov S. A., Terekhov V. A., Domashevskaya E. P. Influence of a weak pulsed electromagnetic field on the atomic structure of natural aluminosilicates clinoptilolite, montmorillonite and palygorskit. *Kondensirovannye sredy i mezhfaznye granitsy = Condensed Matter and Interphases*. 2020;22(2): 18–27. DOI: https://doi.org/10.17308/kcmf.2020.22/2525

1. Introduction

In the 70s of the last century it was established experimentally that electromagnetic treatment quite strongly affects the hydration of ions. Significant changes in ion hydration are observed in dilute solutions in which structural stabilizer ions are present: ions capable of forming complexes with water (Ni^{2+}, Cu^{2+}, Fe^{3+}) and the most hydrophilic ions (Ca^{2+}, Mg^{2+}, Li^{+}) [1–4]. A different change in the hydration of para- and diamagnetic ions can be tried to be associated with a change in the structure of

✉ Domashevskaya Evelina Pavlovna, e-mail: ftt@phys.vsu.ru

water. There are many facts confirming the weak changes that occur in water systems after exposure to weak electromagnetic pulses [3, 4]. First of all, water molecules are affected by weak magnetic fields, the connection of which with other molecules is somehow weakened. Molecules that retain strong hydrogen bonds are most easily exposed.

When an external magnetic field is applied to diamagnetic materials, one should first of all expect orientational effects of extended supramolecular structures and macromolecules due to the large anisotropy of the diamagnetic susceptibility of these formations in accordance with the prevailing ideas about the primary mechanisms of the magnetic field action on matter. When an external magnetic field is applied to diamagnetic materials, one should first of all expect orientational effects of extended polymer supramolecular structures and macromolecules due to the large anisotropy of the diamagnetic susceptibility of these formations in accordance with prevailing ideas about the primary mechanisms of the magnetic field on a substance.

The influence of weak electromagnetic pulses can be traced in aqueous systems by some changes in their physicochemical and physical properties. The change in the properties of a homogeneous liquid phase is insignificant. To a greater extent, magnetic treatment affects processes associated with phase transformations or heterogeneous water systems [3, 4]. The resulting effects are already more noticeable (in contrast to changes in the homogeneous liquid phase) and will remain for a long time. The results of studies of the hydration properties of clinoptilolite and glaukeonite from the group of aluminosilicates showed [5] that at relatively low electromagnetic field intensities, i.e. Under the influence of the so-called weak magnetic fields, the sorption capacity and specific surface area of the samples significantly increase, which is more noticeable for dilute solutions. At high electromagnetic fields, the effect decreases and becomes the opposite.

Aluminosilicates are one of the large groups of minerals, which, in turn, is included in the class of silicates. Simply put, silicates contain silicon and aluminum oxides. Natural species of this group are minerals located in the earth's crust. However, there is the possibility of obtaining them chemically using hydrothermal synthesis, simulating the natural geochemical processes that occur in an environment of superheated aqueous solutions under pressure.

The structural features of zeolites make it possible to modify their aluminosilicate properties by various methods without destroying their crystalline structure, while the modified structures expand the range of potential applications.

The difference between aluminosilicates and silicates is that silicon and aluminum have tetrahedral coordination in them, and part of the silicon in the aluminosilicate is replaced by aluminum and/or Na, K, Ca impurity atoms (Fig. 1). Silicon-oxygen and aluminum-oxygen tetrahedra, in turn, are interconnected by a common oxygen atom (oxygen Si-O-Si (Al) bridge bonds), and this bond is formed by flat grids, chains, ribbons, rings, three-dimensional frameworks [6].

These features of the atomic structure of natural and artificial aluminosilicates allow their use in medicine, food and chemical industries, in agriculture, as molecular sieves, catalysts, in water purification, fine purification and separation of gases, in the chromatographic analysis of gases and liquids, etc.

The aim of this work is to study possible changes in the atomic and electronic structure after exposure to a weak pulsed electromagnetic field on the atomic structure of natural aluminosilicates in the form of clinoptilolite, montmorillonite and palygorskite minerals by X-ray diffraction and ultra-soft X-ray spectroscopy methods.

2. Objects and methods of research

The objects of study of the weak pulsed electromagnetic field (WPEMF) influence were powdered samples of three aluminosilicate minerals. One of them, clinoptilolite has a rigid skeleton structure, its chemical formula is $KNa_2Ca_2(Si_{29}Al_7)O_{72}\cdot 24H_2O$. It is an aluminosilicate of monoclinic syngony with a C2/m space group and unit cell parameters: a = 17.671 Å, b = 17.912 Å, c = 7.410 Å, $\alpha = 90°$, $\beta = 91.59°$, $\gamma = 90°$ [7].

The next montmorillonite sample has a layered expanding structure and no less

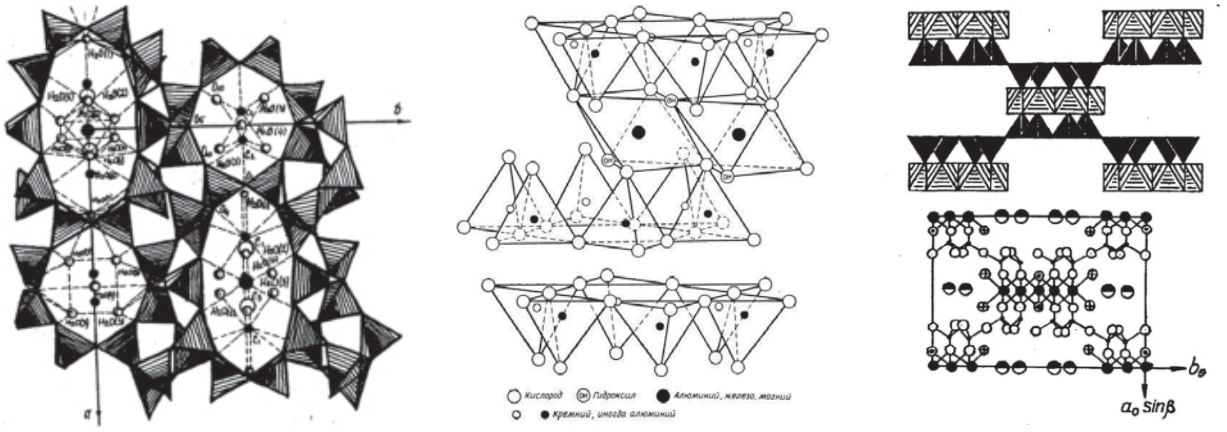

a *b* *c*

Fig. 1. Schematic representation of structures: a) clinoptilolite; b) montmorillonite; c) palygorskite

complex chemical formula $Ca_{0.2}(AlMg)_2Si_4O_{10}(OH)_2 \cdot 4H_2O$, the components of which form a hexagonal crystal lattice with parameters a = 5.169 Å, b = 5.169 Å, c = 15.02 Å, α = 90°, β = 90°, γ = 120° [8].

The third palygorskite sample has the chemical formula $MgAlSi_4O_{10}(OH) \cdot 4H_2O$ [9], different from the two aluminosilicates above, and the layered ribbon structure of the monoclinic syngony with the Pn space group and unit cell parameters a = 17. 864 Å, b = 12.681 Å, c = 5. 127 Å, α = 90°, β = 92.23°, γ = 90° [9].

The setting for creating weak pulsed electromagnetic fields (WPEMF) consists of four main parts: an energy source, energy storage, key and solenoid. The pulse generator provides the amplitude of the magnetic field from 0.5 to 120 mT. The pulse shape is half-sinusoidal. The exposure parameters are as follows: magnetic induction – 71 mT, pulse repetition period T – 10 ms; pulse supply frequency f – 100 Hz, pulse exposure time – 30 sec. For electromagnetic impulse treatment, a bucks with a powder of aluminosilicate of a certain mass were placed inside a solenoid, to which a current was applied to create an electromagnetic field.

Samples of the three listed powdered minerals both in the initial state and 48 hours after WPEMF exposure were studied by X-ray diffraction (XRD) and ultra-soft X-ray spectroscopy (USXES) methods.

X-ray phase analysis of the samples before and after irradiation was carried out on a diffractometer DRON-4-07 with X-ray radiation Co$K\alpha$, λ = 1.69 Å.

The distribution of the state of the valence electrons of silicon and aluminum in the valence band of the studied minerals before and after irradiation was analyzed by the energy distribution of the local partial density of the Si and Al valence states by ultra-soft X-ray emission spectroscopy (USXES) method on a RSM-500 laboratory X-ray spectrometer-monochromator [10–12]. X-ray emission Si and Al $L_{2,3}$-spectra were obtained upon excitation by electrons with an energy of 3 keV, corresponding to a sample analysis depth of 60 nm [11–13].

3. Results and discussion

3.1. X-ray diffraction

X-ray diffraction data show on Figures 2–4 the diffraction patterns from powder samples of three minerals obtained before (upper gray curves) and 48 hours after WPEMF irradiation (lower black curves).

Tables 1–3 show the values of interplanar distances d (Å) and intensities I (%) of Bragg reflections from the studied samples in comparison with the corresponding values for minerals from the International Center for Diffraction Data (ICDD) PDF Card 2012 (last columns). Of the numerous PDF ICDD maps of various modifications of each of the minerals, maps with d (Å) and I (%) values that were closest to our data were selected for comparison. Some differences even of these closest data from ours can be explained by the presence in the minerals of impurities characteristic of this deposit.

Comparison of d (Å) and I (%) obtained before and after WPEMF irradiation presented in

Figures 2–4 and Tables 1–3 shows that the vast majority of Bragg reflections characterizing one or another phase of aluminosilicates of each mineral retain position on the 2θ° scale and relative intensities. However, some weak reflections were better manifested or even appeared after WPEMF irradiation.

So, in the diffractogram of clinoptilolite (Fig. 2 and Table 1) after irradiation, two reflections appeared, corresponding to d = 4.261 Å and d = 4.040 Å, which are absent not only in the initial sample, but also in the sample from the ICDD database [7].

After irradiation of the sample, two reflections also appeared on the diffractogram of montmorillonite (Fig. 3 and Table 1), corresponding to d = 3.408 Å and d = 3.240 Å, one of which is missing in the comparison sample from the ICDD database [8].

And only on the diffraction pattern of palygorskite (Fig. 4) after irradiation did one weak reflection appear, corresponding to d = 1.973 Å (I = 10 %), which is present in the comparison sample with a barely noticeable intensity d = 1.964 Å (I = 1%) [8].

All these data indicate that a weak pulsed electromagnetic field affects the atomic structure of the crystal lattices of powdered natural minerals, clinoptilolite, montmorillonite and palygorskite, a slight deformation of which leads to the appearance of one or two additional superstructural diffraction lines.

3.2. Ultra-soft X-ray emission Si $L_{2,3}$ spectra of silicon

In solids of any composition under the influence of electronic or quantum excitation, electronic transitions arise from the valence band to vacancies in the core shells of all atoms of studied material with the formation of the characteristic X-ray emission valence bands (XEVB). The XEVB for elements of the third period, which include silicon and aluminum of minerals from the class of aluminosilicates, refers to the region of the ultra-soft X-ray spectrum (USXES) with nanometer wavelengths

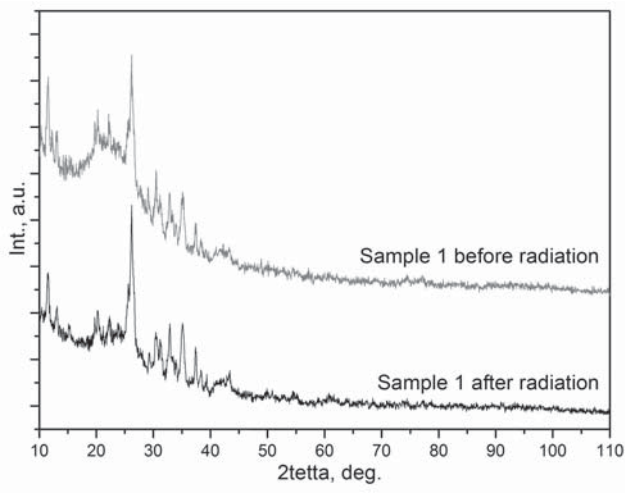

Fig. 2. Diffraction patterns of clinoptilolite (Sample 1) before (upper gray curve) and after WPEMF irradiation (lower black curve)

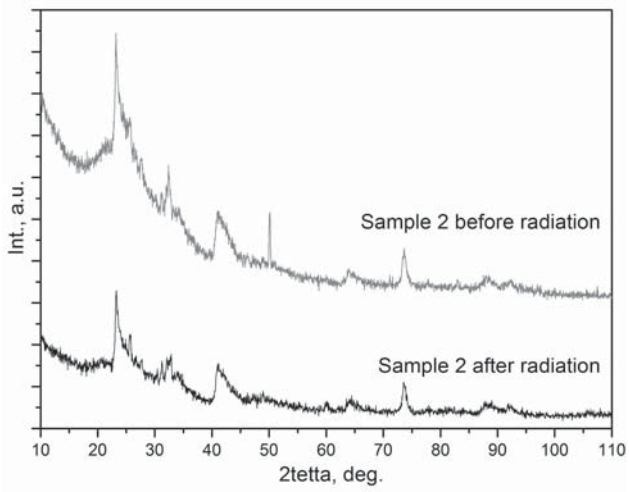

Fig. 3. Diffraction patterns of montmorillonite (Sample 2) before (upper gray curve) and after WPEMF irradiation (lower black curve)

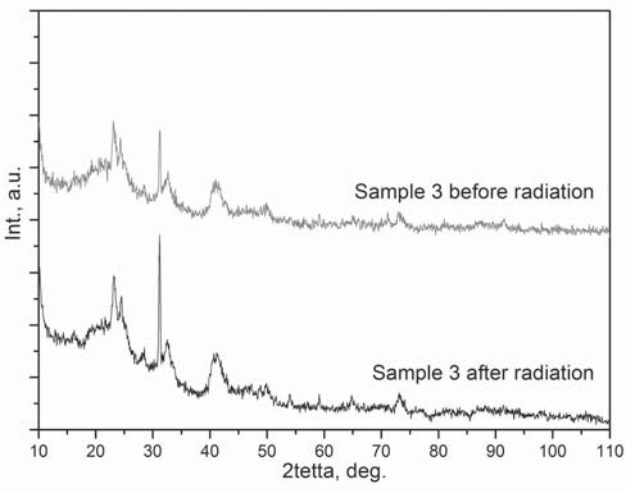

Fig. 4. Diffractograms of palygorskite (Sample 3) before (upper gray curve) and after WPEMF irradiation (lower black curve)

Table 1. The values of interplanar distances *d* (Å) and intensities *I* (%) for clinoptillolite samples before and after WPEMF irradiation in comparison with PDF Card 00-039-1383 [8] for monoclinic clinoptilolite Clinoptillolite-Ca C2/m, *a* = 15.838 Å, *b* = 17.912 Å, *c* = 7.410 Å, α = 90°, β = 91.59°, γ = 90° [7]

No.	Before irradiation		After irradiation		PDF 2012 00-039-1383 Clinoptillolite-Ca [7]	
	d, Å	Int. *I* (%)	*d*, Å	Int. *I* (%)	*d*, Å	Int. *I* (%)
1	9.972	22	9.829	7		
2	**8.896**	**63**	**8.896**	**33**	**8.950 (020)**	**100**
3	8.423	23				
4	7.817	25	7.847	15	7.930 (200)	13
5	6.746	12	6.790	11	6.780 (20-1)	9
6					5.940 (220)	3
7					5.590 (130)	5
8	5.219	43	5.232	20	5.240 (31-1)	10
9	5.092	53	5.117	22	5.120 (111)	12
10			4.866	14		
11	4.659	51	4.628	21	4.650 (13-1)	19
12	4.314	31	4.350	17	4.350 (40-1)	5
13			4.261	15		
14			4.040	45		
15					3.976 (131)	61
16	**3.949**	**100**	**3.949**	**100**	**3.955 (330)**	**63**
17					3.905 (240)	48
18					3.835 (221)	7
19					3.738 (24-1)	6
20					3.707 (041)	5
21	3.569	20	3.545	12	3.554 (31-2)	9
22	3.408	41	3.408	27	3.424 (22-2)	18
23	3.398	40			3.392 (40-2)	12
24	3.333	22	3.333	23	3.316 (002)	6
25	3.170	32	3.161	36	3.170 (42-2)	16
26			3.066	13	3.074 (13-2)	9
27					2.998 (35-1)	18
28	**2.968**	**41**	**2.964**	**40**	**2.971 (151)**	**47**
29	2.785	23	2.792	26	2.795 (62-1)	16
30	2.725	12	2.725	13	2.730 (26-1)	16
31			2.659	12	2.667 (202)	4

Table 2. The values of interplanar distances *d* (Å) and intensities *I* (%) for montmorillonite samples before and after irradiation in comparison with PDF Card 00-013-0135 [8], for hexagonal montmorillonite-15A: *a* = 5.169 Å, *b* = 5.169 Å, *c* = 15.02 Å, α = 90°, β = 90°, γ = 120° [8]

No.	Before irradiation		After irradiation		PDF 2012 00-013-0135 Montmorillonite-15A [8]	
	d, Å	Int. *I*, %	*d*, Å	Int. *I*, %	*d*, Å	Int. *I*, %
1					15.00 (001)	100
2					5.01 (003)	60
3	**4.451**	**100**	**4.442**	**100**	**4.50 (100)**	**80**
4	4.043	30	4.025	50		
5					3.77 (004)	20
6			3.408	14	3.50	10
7	3.337	10	3.323	26	3.30 (103)	10
8			3.240	*38*		
9	3.208	36	3.166	50	3.02 (005)	60
10	2.550	34	2.547	16	2.58 (110)	40
11					2.50 (006)	40
12	2.112	40	2.161	19	2.26 (200)	10
13					1.88 (008)	10
14	1.689	15	1.679	39	1.70 (210)	30
15					1.50 (00 10)	50
16	1.494	29	1.495	15	1.493 (300)	50
17	1.289	10	1.277	10	1.285 (221)	20
18	1.240	5			1.243 (310)	20

Table 3. The values of interplanar distances *d* (Å) and intensities *I* (%) for palygorskite samples before and after irradiation in comparison with PDF Card 2012 00-029-0855 [9] for monoclinic palygorskite Pn: *a* = 17. 864 Å, *b* = 12.681 Å, *c* = 5.127 Å, α = 90°, β = 92.23°, γ = 90° [9]

No.	Before irradiation		After irradiation		PDF 2012 00-029-0855 Palygorskite [9]	
	d, Å	Int. *I*, %	*d*, Å	Int., *I* %	*d*, Å	Int. *I*, %
1	**10.010**	**100**	**10.000**	**100**	**10.34 (110)**	**100**
2					**6.34 (020)**	**15**
3					5.38 (310)	7
4	**4.440**	**100**	**4.461**	**52**	4.47 (400)	8
5	4.237	40	4.219	37	4.27 (-211)	3
6					4.11 (130)	3
7					3.95 (-301)	1
8					3.65 (420)	4
9					3.45 (330)	1
10	**3.323**	**82**	**3.328**	**100**	3.35 (-321)	2
11					3.230 (-131)	3
12	3.228	32	3.199	25	**3.170 (040)**	**10**
13	2.535	51	2.547	30	2.536 (050)	6
14	2.122	17	2.121	10	2.113 (060)	1
15			*1.973*	*10*	1.964 (910)	1
16	1.814	22	1.815	10	1.814 (070)	1
17	1.662	10	1.672	10	1.672 (271)	1
18	1.501	26	1.502	14	1.507 (181)	2
19					1.488 (12 00)	2

and energies of up to several hundred electron volts, measured from the zero Fermi level. In this case, the distribution of the spectrum intensity of each element carries information on the local density of valence states near atoms of a given sort [10–13]. Sensitivity to changes in the chemical environment of the radiating atom is an advantage of X-ray emission spectroscopy. By changes of the XEVB fine structure, one can judge the change in the nearest environment, which allows not only elemental, but even phase analysis of the samples [14, 15]. And since in the study of REP the transition is used the valence bande-core level transitions, the advantage of the UMRES method is the relative simplicity of interpreting the compared to optical band-band spectra [10–13].

As for the basic elements of the three minerals of the group of aluminosilicates, silicon and aluminum, first in Fig. 5 we presented the Al L2,3 aluminum spectra and Si Si L2,3 spectra of all three clinoptilolite samples recorded in a single energy scale successively (Sample 1), montmorillonite (Sample 2) and palygorskite (Sample 3) before and after exposure to a weak pulsed electromagnetic field (71 mTl). The upper spectra in this figure belong to the reference SiO_2 and Al_2O_3 samples.

In the dipole approximation of the selection rules for X-ray transitions, the Si $L_{2,3}$- and Al $L_{2,3}$-spectra reflect the density distribution of the 3s, p (d) states of these elements in the valence band of the corresponding minerals. In this case, the second high-energy main maximum of these spectra corresponds to the hybridization of valence 3s, p-states with O 2p-states of oxygen, i.e. reflects ion-covalent bonds of silicon-oxygen and aluminum-oxygen tetrahedral bonds.

When analyzing the spectra in Fig. 5, we immediately note only a slight increase in intensity in the range 60–72 eV compared to the background at the site of the aluminum Al $L_{2.3}$ spectra compared to the intense silicon Si $L_{2.3}$ band. This circumstance is associated primarily with a significantly lower aluminum content compared to silicon in the chemical formulas of all the studied minerals. The next noticeable increase in intensity with a maximum at 76 eV corresponds to the so-called long-wave / low-energy satellite Si $L_{2,3}$ spectrum, which reflects the interaction of Si 3s, p + O 2s in the O 2s oxygen subband, i.e. due to the amount of oxygen bound to silicon. An increase in the intensity in this region of the weak palygarskite spectrum is due to the superposition of the Cu M2.3 spectrum of copper, from which the sample holder is made.

In the following Figures 6–8, we present separately for each mineral the results of modeling

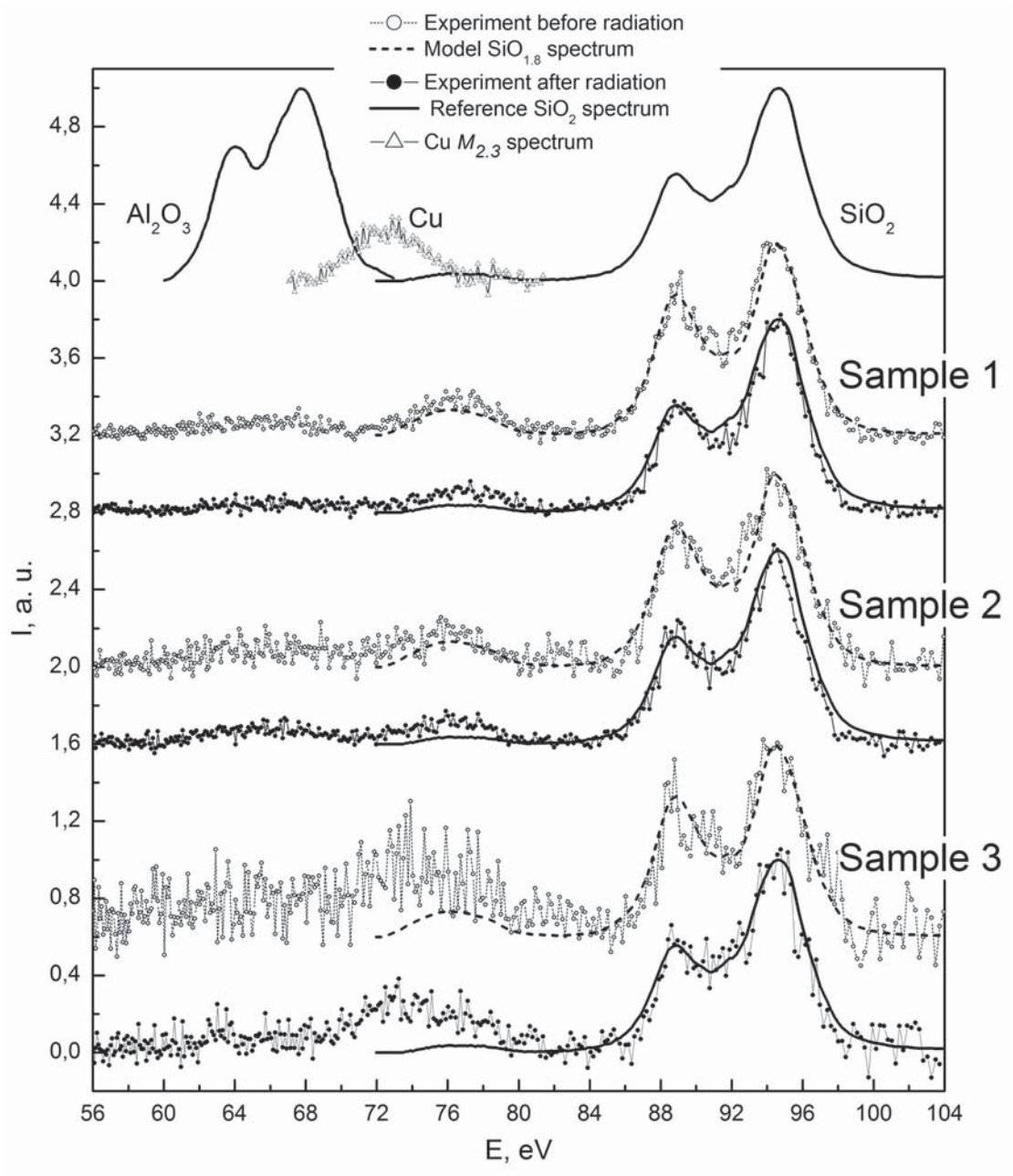

Fig. 5. USXES Al $L_{2,3}$ and Si $L_{2,3}$ spectra of clinoptilolite (Sample 1), montmorillonite (Sample 2) and palygorskite (Sample 3) before (thin lines with circles) and after WPEMF irradiation (lines with black dots). The uppermost spectra belong to the reference samples of SiO_2 and Al_2O_3

Si $L_{2,3}$-silicon spectra using reference spectra of silicon suboxides of different compositions and silicon dioxide and subsequent fitting to experimental spectra [14, 15], which was carried out to determine the phase composition silicon oxides in samples before and after exposure toWPEMF.

The simulation results of Si $L_{2,3}$ spectra showed that all initial samples contain only 40 % of the stoichiometric SiO_2 phase, and the remaining 60 % is silicon suboxide $SiO_{1,7}$, which is, in fact, non-stoichiometric dioxide with numerous oxygen vacancies. Thus, the average weighted statistically distributed composition of oxidized silicon in the starting aluminosilicates is $SiO_{1.8}$ = 40 % SiO_2 + 60 % $SiO_{1.7}$.

After WPEMF irradiation (solid lines with black dots in Figs. 6–8), silicon dioxide SiO2 becomes the predominant phase in all samples. Moreover, in the irradiated clinoptilolite (Fig. 6)

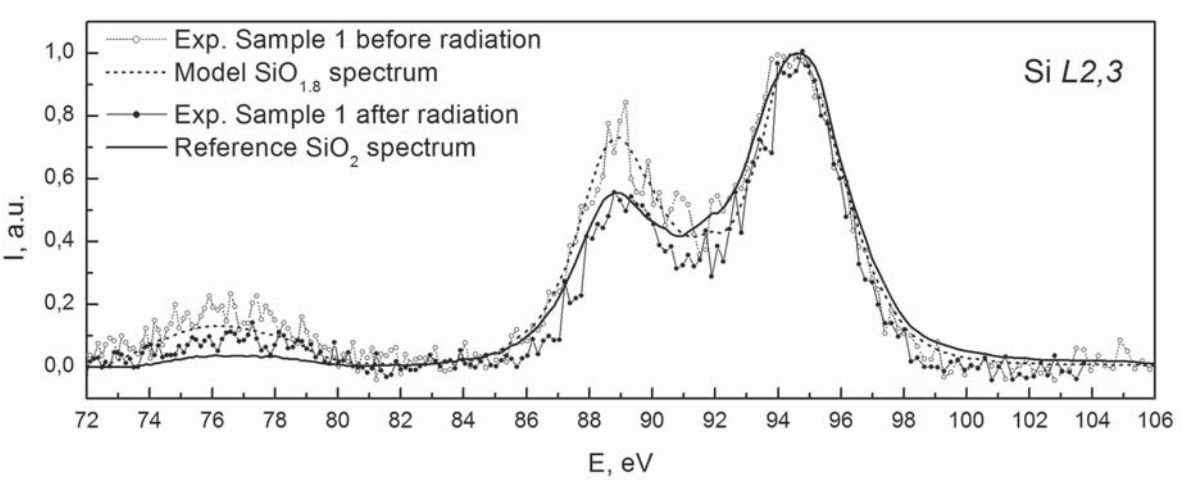

Fig. 6. USXES Si $L_{2,3}$-spectra of clinoptilolite (Sample 1) before (thin line with circles) and after WPEMF irradiation (line with black dots)

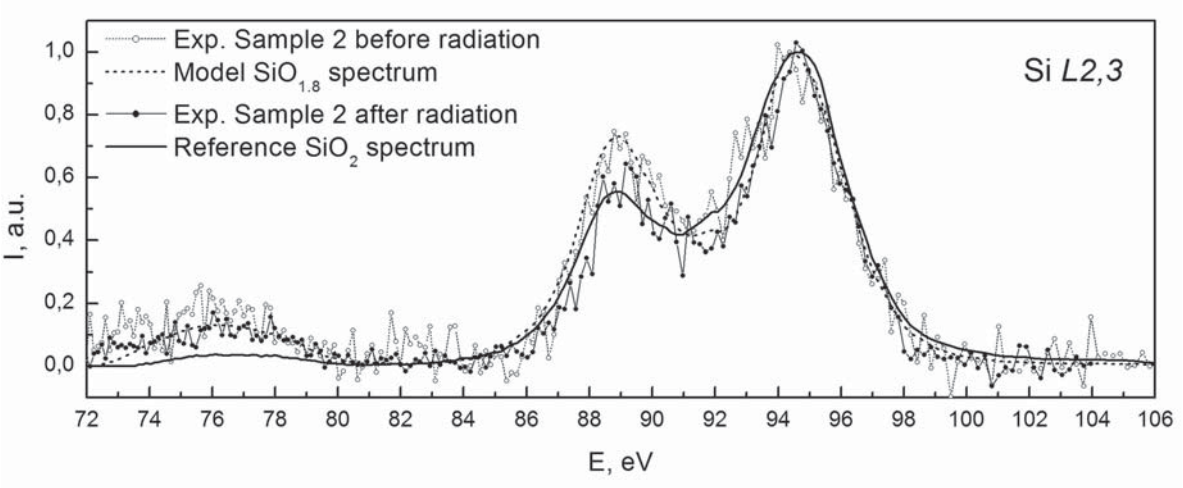

Fig. 7. USXES Si $L_{2,3}$-spectra of montmorillonite (Sample 2) before (thin line with circles) and after WPEMF irradiation (line with black dots)

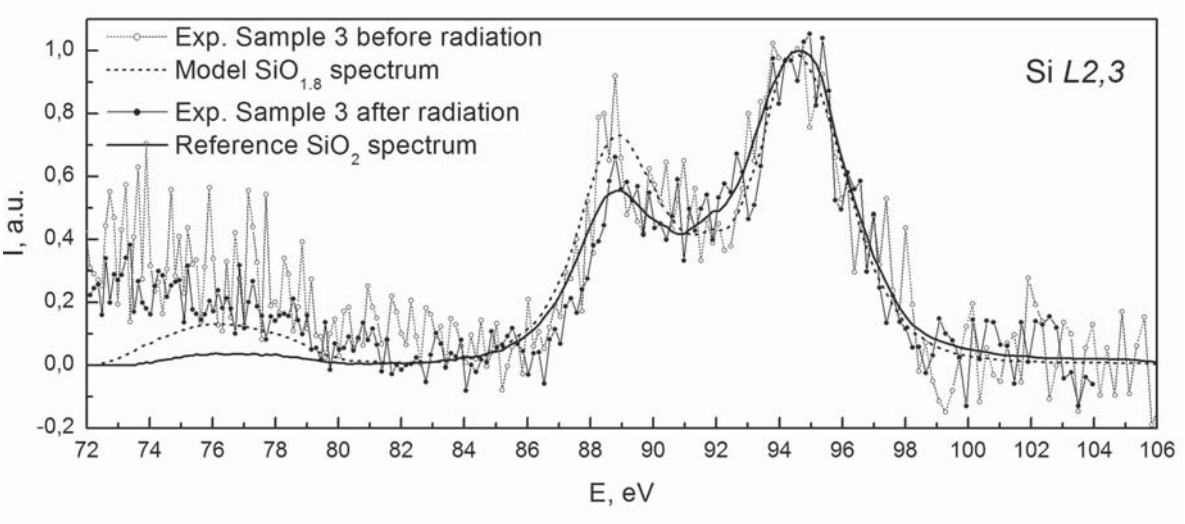

Fig. 8. USXES Si $L_{2,3}$- palygorskite spectra (Sample 3) before (thin line with circles) and after WPEMF irradiation (line with black dots)

and palygorskite (Fig. 8), the stoichiometric SiO_2 phase is unique, and in the irradiated montmorillonite (Fig. 7) its predominance after irradiation rose to 80 %, but did not reach 100 %, as in two other samples.

Nevertheless, a significant healing of defects in the form of numerous oxygen vacancies in the silicon-oxygen tetrahedra of the initial minerals under the influence of WIEMF can occur as a result of the transition of oxygen ions from air adsorbed by the samples, or from superstoichiometric oxygen, from structured water molecules of H_2O or OH groups to vacancy sites.

4. Conclusion

Comparing the experimental results on the effect of a weak pulsed electromagnetic field on the powders of three minerals from the group of natural aluminosilicates that we identified as clinoptilolite [7] $KNa_2Ca_2(Si_{29}Al_7)O_{72}\cdot 24H_2O$, montmorillonite [8] $Ca_{0.2}(AlMg)_2Si_4O_{10}(OH)_2\cdot 4H_2O$, and palygorskite $MgAlSi_4O_{10}(OH)\cdot 4H_2O$ [9], using two different methods of XRD and USXES, we can conclude that both methods, each in its own way, detected noticeable changes in the samples, which persist at least 48 hours after WPEMF irradiation.

The USXES method recorded changes in the local environment of silicon by oxygen atoms with a change in the average stoichiometry from $SiO_{1.8}$ in the initial samples to a near or equal SiO_2. in irradiated samples that occur as a result of filling vacancies in silicon-oxygen tetrahedra with oxygen, most likely from adsorbed air.

Unfortunately, it was not possible to register such changes in aluminum-oxygen tetrahedra due to the low aluminum content in the samples.

Nevertheless, the local short-range order changes observed by the USXES method in the silicon-oxygen tetrahedra affect the atomic structure of entire crystal lattice of all three aluminosilicates, and appear as one or two superstructural lines on the diffractograms of the samples after WPEMF irradiation.

Conflict of interests

The authors declare that they have no known competing financial interests or personal relationships that could have influenced the work reported in this paper.

References

1. Hack E. Z., Rick T. R. O vliyanii postoyannogo magnitnogo polya na kinetiku dvizheniya ionov v vodnykh rastvorakh sil'nykh elektrolitov [On the effect of a constant magnetic field on the kinetics of ion motion in aqueous solutions of strong electrolytes]. *Reports of the Academy of Sciences of the USSR*. 1967;175(4): 856–858. (In Russ.)

2. Martynova O. I., Gusev B. T., Leontiev E. A. K voprosu o mekhanizme vliyaniya magnitnogo polya na vodnye rastvory solei [To the question of the mechanism of the influence of the magnetic field on aqueous solutions of salts]. *Uspekhi Fizicheskikh Nauk*. Успехи физических наук. 1969;98: 25–31. (In Russ.)

3. Chesnokova L. N. *Voprosy teorii i praktiki magnitnoi obrabotki vody i vodnykh sistem* [Questions of the theory and practice of magnetic treatment of water and watersystems]. Moscow: Tsvetmetinformatsiya Publ.; 1971. 75 c.

4. Kronenberg K. Experimental evidence for the effects of magnetic fields on moving water. *IEEE Transactions on Magnetics*. 1985;21(5); 2059–2061. DOI: https://doi.org/10.1109/tmag.1985.1064019

5. Kotova D. L., Artamonova M. I., Krysanova T. A., Vasilenko M. S., Novikova L. A., Belchinskaya L. I., Petukhova G. A. The effect of a pulsed magnetic field on the hydration properties of clinoptilolite and glauconite. *Protection of Metals and Physical Chemistry of Surfaces*. 2018;54(4): 598–602. DOI: https://doi.org/10.1134/S2070205118030073

6. Vernadsky V. I., Kurbatov S. M. *Zemnye silikaty, alyumosilikaty i ikh analogi* [Earth silicates, aluminosilicates and their analogues. 4th ed.]. Moscow – Leningrad Publ.; 1937. 378 p.

7. CPDS – International Center for Diffraction Data. PDF Card 2012 00-039-1383

8. CPDS – International Center for Diffraction Data. PDF Card 2012 00-013-0135

9. CPDS – International Center for Diffraction Data. PDF Card 2012 00-029-0855

10. Zimkina T. M., Fomichev V. A. *Ul'tramyagkaya rentgenovskaya spektroskopiya* [Ultra-soft x-ray spectroscopy]. Leningrad: Leningrad State University Publ.; 1971. 132 p.

11. Shulakov A. S., Stepanov A. P. *Glubina generatsii ul'tramyagkogo rentgenovskogo izlucheniya v SiO_2* [Ultrasoft X-ray Generation Depth in SiO_2]. *Physics, Chemistry and Mechanics of Surfaces*. 1988;10: 146–150. (in Russ.)

12. Terekhov V. A., Trostyansky S. N., Seleznev A. E., Domashevskaya E. P. Izmenenie plotnosti lokalizovannykh sostoyanii v poverkhnostnykh sloyakh amorfnogo gidrogenezirovannogo kremniya pri vakuumtermicheskikh otzhigakh [The change in the density of localized states in the surface layers of

amorphous hydrogenated silicon during vacuum thermal annealing] *Physics, Chemistry and Mechanics of Surfaces*. 1988;5: 74-80.

13. Domashevskaya E. P., Peshkov Y. A , Terekhov V. A., Yurakov Y. A., Barkov K. A. Phase composition of the buried silicon interlayers in the amorphous multilayer nanostructures $[(Co_{45}Fe_{45}Zr_{10})/a\text{-Si:H}]_{41}$ and $[(Co_{45}Fe_{45}Zr_{10})_{35}(Al_2O_3)_{65}/a\text{-Si:H}]_{41}$. *Surf. Interface Anal.* 2018;50(12–13): 1265–1270. DOI: https://doi.org/10.1002/sia.6515

14. Manukovsky E. Yu. Elektronnaya struktura, sostav i fotolyuminestsentsiya poristogo kremniya [Electronic structure, composition and photoluminescence of porous]. *Abstract of the candidate's thesis.* Voronezh: Voronezh State University; 2000. 16 p.

15. Domashevskaya E. P., Terekhov V. A., Turishchev S. Yu., Przhimov A. S., Kharin A. N., Parinova E. V, Rumyantseva N. A., Usoltseva D. S., Fomenko Yu. L., Belenko S. V. Atomic and electronic structure of amorphous and nanocrystalline layers of semi-insulating silicon obtained by chemical deposition at low pressure. *Journal of Surface Investigation: X-Ray, Synchrotron and Neutron Techniques*. 2015;6(6): 1228–1236. DOI: https://doi.org/10.1134/S1027451015060257

Information about the authors

Larisa I. Belchinskaya, DSc in Technical Sciences, Professor, Voronezh State Forestry University named after G. F. Morozov, Voronezh, Russian Federation; e-mail: chem@vglta.vrn.ru. ORCID iD: http://orcid.org/0000-0003-3921-8018.

Konstantin V. Zhuzhukin, postgraduate student, Voronezh State Forestry University named after G. F. Morozov, Voronezh, Russian Federation; e-mail: chem@vglta.vrn.ru. ORCID iD https://orcid.org/0000-0002-7093-3274.

Konstantin A. Barkov, postgraduate student, Head of the Laboratory, Department of Solid State Physics and Nanostructures, Voronezh State University, Voronezh, Russian Federation; e-mail: barkov@phys.vsu.ru. ORCID iD: https://orcid.org/0000-0001-8290-1088.

Sergey A. Ivkov, postgraduate, Leading Electronics, Voronezh State University, Voronezh, Russian Federation; e-mail: ivkov@phys.vsu.ru. ORCID iD: https://orcid.org/0000-0003-1658-5579.

Vladimir A. Terekhov, DSc in Physics and Mathematics, Full Professor, Department of Solid State Physics and Nanostructures, Voronezh State University, Voronezh, Russian Federation; e-mail: ftt@phys.vsu.ru. ORCID iD: https://orcid.org/0000-0002-0668-4138.

Evelina P. Domashevskaya, DSc in Physics and Mathematics, Full Professor, Head of the Department of Solid State Physics and Nanostructures, Voronezh State University, Voronezh, Russian Federation; e-mail: ftt@phys.vsu.ru. ORCID iD: https://orcid.org/0000-0002-6354-4799.

All authors have read and approved the final manuscript.

Translated by Valentina Mittova.
Edited and proofread by Simon Cox.